

Focus+context exploration of hierarchical embeddings

Hollt, T.; Vilanova, A.; Pezzotti, N.; Lelieveldt, Boudewijn; Hauser, H.

DOI

[10.1111/cgf.13711](https://doi.org/10.1111/cgf.13711)

Publication date

2019

Document Version

Final published version

Published in

Computer Graphics Forum

Citation (APA)

Hollt, T., Vilanova, A., Pezzotti, N., Lelieveldt, B., & Hauser, H. (2019). Focus+context exploration of hierarchical embeddings. *Computer Graphics Forum*, 38(3), 569-579. <https://doi.org/10.1111/cgf.13711>

Important note

To cite this publication, please use the final published version (if applicable). Please check the document version above.

Copyright

Other than for strictly personal use, it is not permitted to download, forward or distribute the text or part of it, without the consent of the author(s) and/or copyright holder(s), unless the work is under an open content license such as Creative Commons.

Takedown policy

Please contact us and provide details if you believe this document breaches copyrights. We will remove access to the work immediately and investigate your claim.

Focus+Context Exploration of Hierarchical Embeddings

T. Höllt^{1,2} , A. Vilanova² , N. Pezzotti² , B.P.F. Lelieveldt³ , and H. Hauser^{2,4,5},

¹Leiden Computational Biology Center, Leiden University Medical Center, The Netherlands

²Computer Graphics and Visualization Department, TU Delft, The Netherlands

³Leiden University Medical Center, LKEB, Department of Radiology, Leiden, The Netherlands

⁴Department of Informatics University of Bergen, Norway

⁵Mohn Medical Imaging and Visualization Center, Bergen, Norway

Abstract

Hierarchical embeddings, such as HSNE, address critical visual and computational scalability issues of traditional techniques for dimensionality reduction. The improved scalability comes at the cost of the need for increased user interaction for exploration. In this paper, we provide a solution for the interactive visual Focus+Context exploration of such embeddings. We explain how to integrate embedding parts from different levels of detail, corresponding to focus and context groups, in a joint visualization. We devise an according interaction model that relates typical semantic operations on a Focus+Context visualization with the according changes in the level-of-detail-hierarchy of the embedding, including also a mode for comparative Focus+Context exploration and extend HSNE to incorporate the presented interaction model. In order to demonstrate the effectiveness of our approach, we present a use case based on the visual exploration of multi-dimensional images.

CCS Concepts

• **Human-centered computing** → **Information visualization; Visualization theory, concepts and paradigms;**

1. Introduction

In order to successfully benefit from the wealth of information in large and complex datasets, interactive visual data exploration and analysis is used in a variety of application areas such as text analysis [MCCD13], fraud detection [LGM*18], machine learning [PHvG*18], and life sciences [OKB*08, LvUH*18]. Multi-dimensional data is often a core challenge in these processes and dimensionality reduction is regularly an essential part of the approach. Fortunately, a plethora of according techniques is available [BG06, vdMH08, EHH12]. However, with ever increasing data-sizes, visualizing a complete dataset in a single plot is often impossible or leads to a lack of detail or overview. Hierarchical techniques can mitigate those problems through an overview first, detail on demand approach and will likely become essential for visual analysis of large high-dimensional data.

A concept called Focus+Context [Mun14, Chapter 14] has been proven effective for multiple level-of-detail visualization in a single plot and has been used for many types of visualization [CKB09]. In essence, different visual encodings are used to separate semantic groups corresponding to an area of interest (*Focus*) and areas that provide *Context*. The original idea focused on transforming the visual space, such as for lens views [Fur99] or by so-called rubber-sheet warping [SSTR93]. Later on, the concept was generalized to use different visual channels besides space, such as opacity or frequency [Hau06] for separating focus and context. Even with extensive work in recent years, to the best of our knowledge, no Focus+Context concept for embeddings has been proposed yet.

In this paper, we now introduce and specify the concept of Focus+Context for the exploration of embeddings with multiple levels of detail (hierarchical embeddings) such as Hierarchical Stochastic Neighbor Embedding (HSNE) [PHL*16] or Hierarchical Point Placement (HiPP) [PM08]. We implement the proposed concept by extending HSNE and show its viability in a use case, showing the interactive exploration of multi-dimensional imaging data. The main contributions of this paper are twofold:

1. We specify the concept of Focus+Context for embeddings with multiple levels of detail, including the design of
 - a set of interactions supporting the exploration, and
 - a visual representation supporting the distinction of focus and context groups in the embedding.
2. We extend HSNE to support Focus+Context exploration by
 - adapting the creation of the HSNE hierarchy to fit a more fine grained exploration and by
 - specifying multiple modes to define the similarity of points originating from different levels of the hierarchy.

In the following, we first present a requirement analysis for Focus+Context for embeddings (Section 2) and give an overview of the related work (Section 3). In Section 4 we describe our interaction and visualization design, followed by the according extensions to HSNE (Section 5). Then, we present a use case in Section 6 and conclude in Section 7.

2. Problem Description

First, let us briefly define hierarchical embeddings. A hierarchical embedding is a special type of embedding of high-dimensional data in a low-dimensional (e.g., two-dimensional) space. Instead of limiting the embedding to a single mapping, a hierarchy, consisting of n levels $\mathcal{L}^0 \dots \mathcal{L}^{n-1}$, is defined on the input data. Here, \mathcal{L}^0 contains the complete dataset, while every level \mathcal{L}^{k+1} is less detailed than the previous level \mathcal{L}^k . An element $L_i^{k+1} \in \mathcal{L}^{k+1}$, called a landmark, represents (\rightarrow) a set of elements $\{L_j^k \mid L_j^k \leftarrow L_i^{k+1}\} \subset \mathcal{L}^k$. Similarly, we define \rightarrow on sets, i.e. a set \mathcal{S}^{k+1} represents a set on the more detailed level \mathcal{S}^k by the union of the sets represented by its elements

$$\mathcal{S}^k = \bigcup_{\mathcal{S}^{k+1}} \{L_i^k \mid L_i^k \leftarrow L_j^{k+1} \text{ and } L_j^{k+1} \in \mathcal{S}^{k+1}\}.$$

Typically, representation is achieved by aggregation or selection. With the hierarchy defined, the embedding is then defined as a set of mappings, one for each level of the hierarchy. Existing examples of hierarchical embeddings include HSNE [PHL*16] and HiPP [PNML08]. Other forms of hierarchical data representation (e.g. through hierarchical clustering) with mappings in levels (e.g. t-SNE per level) are certainly also viable.

Methods like HSNE [PHL*16] enable an interactive exploration of the hierarchical representation. Usually, the exploration starts on the highest level $n - 1$ of the hierarchy. The analyst can then select any subset $\mathcal{S}^{n-1} \subset \mathcal{L}^{n-1}$ and request a new plot that will contain all elements $\mathcal{S}^{n-2} \subset \mathcal{L}^{n-2}$, represented by the elements in \mathcal{S}^{n-1} . Typical exploration paths can roughly be divided into three groups, illustrated in Figure 1. In the most simple case, the analyst is interested in a specific, large part of the data, separated on the highest level of the hierarchy as \mathcal{S}^{n-1} . Once the analyst has identified this group they typically zoom into this group several times, until a desired level of detail \mathcal{S}^{n-m} with $0 < m \leq n$ is reached (Figure 1a). If the part of the data that is of interest is small and not directly identifiable or separable at the top level of the hierarchy, the analyst zooms into a superset \mathcal{S}^{n-1} of this group $\mathcal{G}^{n-1} \subset \mathcal{S}^{n-1}$ and then recursively zooms into smaller and smaller subsets (Figure 1b) until \mathcal{G}^{n-m} can be separated. In case the analyst wants to compare groups, they can use any combination of the aforementioned strategies to zoom into two groups, \mathcal{G}_1^k and \mathcal{G}_2^k , and compare their structure on the same level k (Figure 1c).

Every such selection and zoom operation leads to a new plot, each limited to a single level of detail (LoD). As a result, multiple disconnected plots separating the data of interest from the context

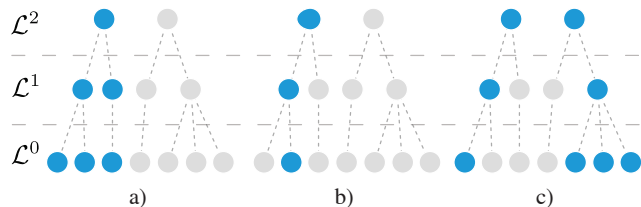


Figure 1: Illustration of Typical Exploration Paths for hierarchical embeddings. Paths indicated by blue nodes in the hierarchy. Repeated zooming into one subset, a), recursive subset selection and zooming, b), and zooming into two groups for comparison, c).

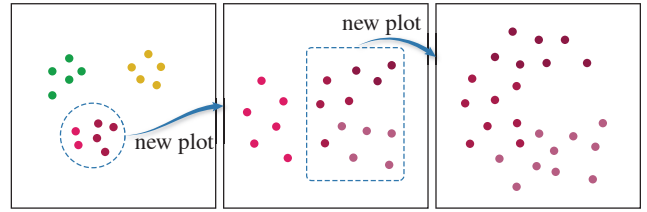


Figure 2: Illustration of an Exploration of a hierarchical embedding through a set of disconnected plots/views.

are created during a typical exploration session (compare Figure 2). Such an interaction is typical for coordinated multiple views with shared data as described by Munzner [Mun14, chapter 13], but can impose a substantial cognitive load as “users are more likely to lose track of their location”. Previously [HPvU*18], we approached this problem by offering a “meta-visualization” that collects the separate plots and augments them with information that guides the exploration. This approach relies on at least two plots, the collection plot and the main embedding where the context is lost.

Here, we now propose to use Focus+Context concepts to enable the exploration of the hierarchy through a single, interactive plot. In brief, instead of zooming into a selection in a separate plot, the analyst creates a *focus*, i.e., a data group of interest, for which more detail is added from the next level(s) of the hierarchy – directly in the same plot. The remaining data points (the *context*) are kept in the plot, but in a de-emphasized style and with less visualization space provided to them. This approach requires less working memory from the users and therefore reduces their cognitive load. To enable the main strategies for exploration as illustrated above, we make use of multiple context groups at different levels of detail. By adding a second focus group, similar to the polyfocal lenses presented by Wang et al. [WWZ*19], we also enable comparative visualization. Since comparative visualization has certain specific requirements, we separate between standard Focus+Context and comparative Focus+Context throughout the manuscript.

Our new solution responds to the following requirements for the interactions (I1 – I9), as well as for the visualization (V1 – V4), which need to be met to support an effective exploration of hierarchical embeddings using Focus+Context concepts. Generally, the analyst must be able to

- I1 request more detail for all data,
- I2 request less detail for all data, and
- I3 return to the initial state.

For zooming into areas of interest, the analyst needs to be able to

- I4 define an area of interest (focus),
- I5a change the focus to a subset of the current focus,
- I5b change the focus to a different set of points,
- I6 request more detail for the focus, and
- I7 request less detail for the focus.

To support a comparative analysis, all of the above need to be implemented with the addition of the possibility to

- I8 create a second focus for comparison and to
- I9 resolve the second focus.

Fulfilling these requirements, we can support all of the above illustrated exploration paths. By adding requirements I2, I3, I7, and

I9, enabling the reversal of other interactions, we provide a fluid traversal of the hierarchy in both directions and consequently multiple successive exploration paths. To support the analyst in the exploration, we consider the following characteristics as relevant for the visual design:

- V1** the focus must use extended space in the visualization,
- V2** the focus must be separated from the context,
- V3** connections between focus and context should be maintained,
- V4** different hierarchy levels must be identifiable.

Requirements **V2** and **V3** are competing. Sometimes the analyst might desire a clear separation between focus and context (**V2**), for example when focussing on an already separated region in the embedding (Figure 2, left). Providing a clear separation between focus and context will then further improve the separation of the cluster. In other cases, however, it might be desired that connections between data points of different levels of detail are maintained, at least to a certain degree (**V3**). For example, when there is no strong separation between data points that are to be assigned to separate groups (Figure 2, middle). In such a case a mapping that respects the connections between data points, while providing some separation, is desired.

3. Related Work

Munzner [Mun14, Chapter 14], as well as Cockburn et al. [CKB09] give an overview of Focus+Context visualization for data exploration. Focus+Context is an established concept to improve exploration of large and complex data. To the best of our knowledge this is the first approach that applies Focus+Context to the exploration of embeddings of high dimensional data. Sedlmayr et al. [SMT13] derive guidelines on the visualization of dimensionality reduced data from an empirical user study. Brehmer et al. [BSIM14] present a task analysis for dimensionality reduction based on interviews with analysts. Finally, Sacha et al. [SZS*17] provide an overview of typical interaction patterns for dimensionality reduction visualizations through an in depth analysis of 58 papers on dimensionality reduction in typical visual workflows.

While single-level-of-detail dimensionality reduction techniques are ubiquitous, the number of hierarchical techniques is limited. HSNE [PHL*16] builds a hierarchy, by selecting representative data-points at different levels of detail, and represents the similarity at each level according to the underlying data. In its original conception, the hierarchy is then explored top to bottom, starting with a complete embedding of the lowest detail level. More and more detailed embeddings are then computed, based on user-selected subsets of the data, and visualized in disconnected views. Previously, we added a hierarchy view [HPvU*18] to the concept that collects all plots in a single visualization. HiPP [PM08] uses Least-Square Projection [PNML08] to map the data to a low dimensional space. The mapped data is then hierarchically clustered and can be visualized at different levels of detail. While this method also allows for in-place expansion of selected groups it does not provide an importance driven assignment of the visual space. Instead the layout is largely identical for different levels of detail, driven by the point placement on the most detailed level. Sparse Multi-Dimensional Scaling (MDS) [SBT04] and MDSteer [WM04] are extension of MDS with a hierarchical data backing. While these techniques

mostly aim at increasing computational performance of the traditional MDS, they could also be adapted to the Focus+Context technique presented in this paper. Approaches for hierarchical PCA exist [WKM98, JPLL01, AEGEALM07], however, they are not a good fit for our proposed technique and the introduced distortion, due to the linear nature of PCA. We have chosen HSNE to implement the Focus+Context concept presented here, as its non-linear nature and flexible and fast hierarchy computation make it a good fit.

4. Focus+Context for Hierarchical Embeddings

As outlined in Section 2, we aim to improve the interpretability of hierarchical embeddings and make their exploration easier through the use of Focus+Context concepts. Figure 3 illustrates the idea of a Focus+Context exploration of a hierarchical embedding. To realize our solution, we make use of two key concepts.

First, let's assume that an embedding is a mapping from a high-dimensional space to a low-dimensional space (here 2D for visualization). Often, this mapping is non-linear. For example, similarity-based embeddings, such as t-SNE [vdMH08], aim to preserve local neighborhoods rather than distances. The main optimization goal is that points that are neighbors in data space should be neighbors in the visualization. While relative distances can provide information about local structure they have little meaning for global structure. Applying Focus+Context techniques to such a plot is then quite natural. We can distort the space between groups without the risk to compromise its interpretation too much, for example, by assigning more visual space to an area of interest (focus). In fact, if we incorporate the notion of Focus+Context regions directly into the mapping, we do not even need to transform the resulting space—instead, the mapping will adapt automatically. As a result, relative local distances will be preserved within a level of detail (LoD) while the analyst only needs to be careful to not compare distances over multiple LoDs. To avoid this pitfall we provide a clear visual separation between different LoDs (requirement **V4**).

Second, while this idea can already improve traditional embeddings with a single LoD, we can mix multiple levels of detail in the same plot by adding a hierarchical representation of the data and the corresponding mappings. This allows a more fine-grained separation between focus and context. We can show the context with little detail while providing more detail for the focus.

Figure 3 illustrates both concepts through three stages of the same exploration as in Figure 2. Note that here the three panels correspond to different stages of the same view, while in Figure 2 they correspond to separate views. The exploration starts with a single LoD on level 2 of a given hierarchy (left). The analyst selects a part of the embedding (left, dashed blue line) as the focus. In the

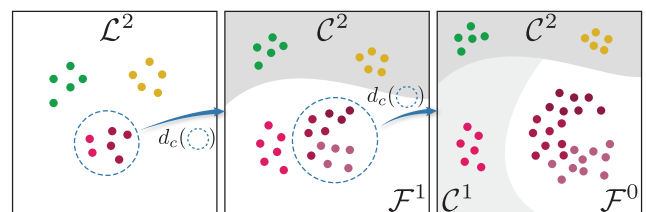


Figure 3: Illustration of a Focus+Context Exploration of a hierarchical embedding in a single view.

next step (middle), the focus region has been expanded, more points have been added from level 1 of the hierarchy. While the number and hierarchy level of points in the context, \mathcal{C}^2 , did not change, the mapping was adjusted to move them slightly to the side and make the representation a bit more compact. The focus, \mathcal{F}^1 , takes more visual space. In the third step, a subset (middle, dashed blue line) of the previous focus was selected as the new focus \mathcal{F}^0 and expanded with data from level 0 (right panel). We now have two context regions, \mathcal{C}^2 and \mathcal{C}^1 , at different LoDs and a detailed focus, \mathcal{F}^0 .

4.1. Interaction Design

To enable the different exploration strategies presented in Section 2, we define a set of interactions fulfilling requirements **I1–I9**. In general, these interactions work on and produce sets of representations of data points. We use the following sets: focus \mathcal{F}^k (comparative focus \mathcal{F}_c^k), as defined on level k of the hierarchy; \mathcal{C}^k stands for the context set on level k ; \mathcal{X}^k corresponds to a selection on level k ; and \mathcal{D} denotes the union of the focus and context sets, active at the current state of the exploration. The new focus and context after the interaction are annotated as \mathcal{F}'^k and \mathcal{C}'^k .

Figure 4 provides an overview of the interactions. Some of the requirements map directly to interactions. As requirements **I1–I3** refer to all data, \mathcal{D} , no additional information is required. We define three according interactions as **(I1)** refine all data, $f(\mathcal{D})$, **(I2)** simplify all data, $s(\mathcal{D})$, and **(I3)** reset all data, $r(\mathcal{D})$.

Requirements **I6** and **I7** are similar in that they operate on a fixed data subset—here, the focus \mathcal{F}^k instead of all data \mathcal{D} . We define two interactions, *differentiate focus more*, $d_+(\mathcal{F}^k)$, and *differentiate focus less*, $d_-(\mathcal{F}^k)$, to fulfill these requirements. As indicated by the term differentiate, these interactions are more general: the goal is to increase or decrease the difference between focus and context. By default, when executing these interactions, we simply request more or less detail for the focus, as required by **I6** and **I7**. However, in some cases, for example when the focus is at the most detailed level, *differentiate focus more* decreases the LoD of the context.

To define or change the focus (requirements **I4**, **I5a**, and **I5b**), the part of the data \mathcal{X}^k that shall become the focus needs to be specified. In practice, the analyst selects \mathcal{X}^k , for example by brushing. Based on contextual information, we can fulfill requirements **I4**, **I5a**, and **I5b** with a single interaction *create focus & differentiate*, $d_c(\mathcal{X}^k)$, that updates the focus and context sets on their corresponding levels in the hierarchy. In any case, we first update the context and then set the new focus to the selection.

All Data		Focus+Context	
$f(\mathcal{D})$	refine	$d_c(\mathcal{X}^k)$	create focus & differentiate
$s(\mathcal{D})$	simplify	$d_+(\mathcal{F}^k)$	differentiate focus more
$r(\mathcal{D})$	reset	$d_-(\mathcal{F}^k)$	differentiate focus less
		$c_c(\mathcal{X}^k)$	create comparative group
		$c_r(\mathcal{F}_c^k)$	resolve comparative group

Figure 4: Scheme of the Proposed Focus+Context Interactions. The left column shows generic interactions, while the right column shows interactions, specific to Focus+Context with interactions for comparative Focus+Context below the dashed line.

If no focus is defined (**I4**), for instance at the beginning of the exploration or after $r(\mathcal{D})$, we can simply define the context as

$$\mathcal{C}'^k := \mathcal{D} \setminus \mathcal{X}^k \quad (1)$$

according to the hierarchy level k on which the user interacted. To fulfill requirements **I5a** and **I5b**, we need to evaluate the selection with respect to the Focus+Context subdivision on which the user interacted and adjust the contexts, accordingly. While selections over multiple LoDs can be implemented by resolving and/or merging the involved sets, we propose to limit selections to a single level of detail for clarity. As a result, we have to consider two potential cases. If the new selection does not overlap with the old focus, $\mathcal{X}^k \cap \mathcal{F}^l = \emptyset$ (**I5b**), it must be part of a less detailed hierarchy level, $l < k$. In this case, the old focus \mathcal{F}^l needs to be reduced in detail to level k , and the resulting \mathcal{F}^k added to the old context without the selection \mathcal{X}^k to create the new context:

$$\mathcal{C}'^k := (\mathcal{C}^k \setminus \mathcal{X}^k) \cup \mathcal{F}^k \quad (2)$$

If $\mathcal{X}^k \subset \mathcal{F}^l$ (**I5a**), it follows that $k = l$ and we can simply add a new context on level k :

$$\mathcal{C}'^k := \mathcal{F}^k \setminus \mathcal{X}^k \quad (3)$$

Note that several context sets can exist on different hierarchy levels. After the context sets are updated, we update the focus in two steps: First, we set the selection as the new focus, $\mathcal{F}'^k := \mathcal{X}^k$. Then, we differentiate the focus by adding the represented data points from the next level, $k - 1$, of the hierarchy:

$$\mathcal{F}'^{k-1} := \{L^{k-1} \mid L^{k-1} \leftarrow \mathcal{F}'^k\} \quad (4)$$

To enable the comparison of two groups (requirements **I8** & **I9**), we define two interactions *create comparative group*, $c_c(\mathcal{X}^k)$, and *resolve comparative group*, $c_r(\mathcal{F}_c^k)$. In principal, $c_c(\mathcal{X}^k)$ works very similar to $d_c(\mathcal{X}^k)$ with the distinction that the comparative focus \mathcal{F}_c must be disjunct from the existing primary focus \mathcal{F} . The same strategy for creating/changing the focus as described above can then also be applied when the user executes $c_c(\mathcal{X}^k)$. To allow a proper structural comparison, we expand \mathcal{F}_c immediately to the same hierarchy level as \mathcal{F} instead of differentiating the new \mathcal{F}_c just once. *Resolve comparative group* maps directly to requirement **I9**. Executing it simply dissolves the comparative focus and merges it into the context group in the hierarchy level it was derived from.

4.1.1. Tree-based Interaction Data Structure

To implement the presented interactions, we propose a tree-based data structure, to track the complete exploration process. A node in the tree represents a semantic group in a given hierarchy level. All leaf nodes combined correspond to the complete data, \mathcal{D} , shown in the Focus+Context plot. Edges in the tree have different interpretations, depending on the number of outgoing edges of a node. If a node has only one outgoing edge, this edge represents an increase in LoD. If a node has more than one outgoing edge the child nodes represent disjunct subgroups of the data points in the parent node (at the same LoD). With this structure, we can implement all (non-comparative) interactions described in Section 4.1.

Reset, $r(\mathcal{D})$, simply cuts all children from the root, returning to the initial state (Figure 5a). Operations that do not change the focus, i.e. $f(\mathcal{D})$, $s(\mathcal{D})$, $d_+(\mathcal{F}^k)$, and $d_-(\mathcal{F}^k)$, simply append a more detailed node to the impacted leaves or remove such leaves.

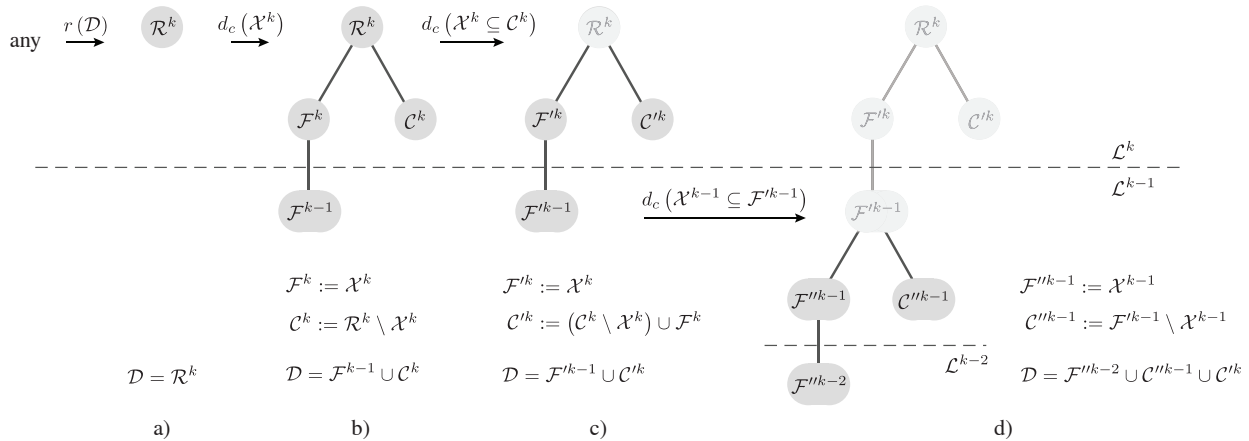


Figure 5: Interactions and their Effect on the Focus+Context Tree. $r(\mathcal{D})$ resets the tree to the root node, a). The result of $d_c(\mathcal{X}^k)$ depends on the selection. If we only have a single node (the root) and the selection is part of the root, a minimal tree is appended, b). If the selection is part of a context, the tree below the first branching node above the corresponding context node is cut off and replaced by the minimal tree, c). Finally, if the selection is part of a focus, a minimal tree is appended to the corresponding focus node, d). Faded nodes indicate no change.

Setting a new focus appends a minimal tree such as the one shown in Figure 5b. As described in Equations 1 to 3, depending on which points are selected, $d_c(\mathcal{X}^k)$ behaves differently. These differences can be translated to slightly different strategies for appending the minimal tree as shown in Figures 5c and 5d. When the selection is a subset of a context group, we replace the parent node of this context with the minimal tree and define the nodes of the template according to Equations 2 and 4 (Figure 5c). When the selection is a subset of the root or current focus, we replace this node with the tree template and define the nodes of the template according to Equations 3 and 4, resulting in stacked context groups (Figure 5d). These template replacements work on any subgraph of arbitrarily complex state graphs of the exploration.

In the case of a comparative Focus+Context exploration, we need to make sure that the primary and the comparative foci are at the same level of detail. Accordingly, the difference between comparative and non-comparative interactions is mostly semantic in the proposed data structure. A comparative focus is created by the same operation on the tree as for creating the primary focus, but followed by as many refine operations as needed to move the comparative focus to the same level of detail as the primary focus. Resolving the secondary focus cuts off the tree at the original branching point.

4.2. Visual Design

As indicated in Section 4, requirements V1–V3 can be naturally met by directly adjusting the mapping of the embedding, instead of transforming the visual space of the embedding plot. Therefore, their execution depends on the choice of the embedding technique. In Section 5, we present how we extended HSNE to support Focus+Context exploration, as well as our extensions to support requirements V1–V3.

Here, we focus on requirement V4 (different hierarchy levels must be identifiable), which can be met universally by augmenting the embedding plot, independent of the type of the embedding. Typically, embeddings are visualized as a scatterplot. In principal, the hierarchy level is a property of each point. However, the visual channels available in a scatterplot, per point (position, color, size,

shape) are usually used to show properties of the data itself. For example, in a typical use case of HSNE [vUHP*17], position is used to indicate the similarity, size to indicate the number of represented data points in the lower hierarchy levels, color to show metadata or the values of one of the original dimensions, and a halo is used to indicate selection status. Since the hierarchy level is the same for all data points within a semantic group and groups shall not intermix (compare requirement V2) we can assume that we can partition the visual space into connected areas of equal LoD. Thus, instead of indicating the LoD per point, we instead use the corresponding regions to indicate the hierarchy level. Particularly, by partitioning the complete visual space, we receive a discrete topographical map where height values correspond to hierarchy levels. We can then use standard methods for visualizing topographical information, such as iso-contours or color-coding to represent the LoD. As illustrated in Figure 3, we use increasingly lighter gray values for the background to indicate increasing LoD. We compute the background in real-time by rendering all points with their respective level mapped to the gray value, followed by an iterative region growing.

5. Focus+Context HSNE

We implemented a prototype of the proposed concept based on Hierarchical Stochastic Neighbor Embedding [PHL*16]. In the following, we give a brief introduction to HSNE (Section 5.1) and present the methodological extensions to the original HSNE in order to support Focus+Context exploration (Section 5.2).

5.1. Background - HSNE

HSNE is a hierarchical dimensionality reduction technique, based on the popular embedding technique t-SNE [vdMH08]. It constructs a hierarchy of so-called landmarks L_i^k , essentially data-points that represent a local neighborhood in a level \mathcal{L}^k of the hierarchy. The set of landmarks forming the most fine-grained level \mathcal{L}^0 equals the set of original data-points. Each subsequent level is then a subset of the previous level ($\mathcal{L}^0 \supset \mathcal{L}^1 \supset \mathcal{L}^2 \supset \dots \supset \mathcal{L}^{n-1}$) with n corresponding to the number of levels. The hierarchy is explored through similarity embeddings, typically starting by embed-

ding all landmarks of the coarsest level \mathcal{L}^{n-1} , followed by selecting a subset of interest $\mathcal{S}^{n-1} \subseteq \mathcal{L}^{n-1}$ and embedding the expanded selection $\mathcal{S}^{n-2} \leftarrow \mathcal{S}^{n-1}$ part of \mathcal{L}^{n-2} . The process is then repeated iteratively, creating multiple disconnected plots. An in-depth description of HSNE is out of the scope of this publication, however, we present the parts that we extend in more detail in the following.

Landmark Selection. The landmarks for level \mathcal{L}^k , $k > 0$, are selected based on their connectivity in level \mathcal{L}^{k-1} . In practice, the connectivity is defined by carrying out a set of random walks on the underlying neighborhood graph. In the original HSNE implementation, a threshold is defined on the number of terminated random walks, to identify the most important landmarks in a data-driven manner. While, the threshold is a parameter that can be adjusted by the user, this is not very intuitive—it is hard to predict and control the number of landmarks on each level and the number of levels needed for a desired reduction. We thus present a modified selection criterion providing better control over the reduction between hierarchy levels in Section 5.2.1.

Landmark Expansion. When zooming into or expanding a set of landmarks \mathcal{S}^k to get more detail, HSNE makes use of a concept called *Area of Influence (AoI)*. To define the AoI of a landmark L_i^k , a second set of random walks is started from each node in \mathcal{L}^{k-1} . When a random walk reaches L_i^k the start node is added to the AoI of L_i^k . The influence $I_{L_i^k}(L_j^{k-1})$ of a landmark $L_i^k \in \mathcal{L}^k$ on a landmark $L_j^{k-1} \in \mathcal{L}^{k-1}$ is defined by the fraction of random walks started at L_j^{k-1} that end in L_i^k .

Ultimately, to expand a selection of landmarks \mathcal{S}^k , we compute the combined influence of all landmarks in the selection on every landmark in \mathcal{L}^{k-1} . The set of landmarks \mathcal{S}^{k-1} corresponding to the expansion of \mathcal{S}^k is then the set of landmarks for which the combined influence of all landmarks in the selection is greater than a predefined threshold γ :

$$\mathcal{S}^{k-1} = \left\{ L_j^{k-1} \mid \sum_{L_i^k \in \mathcal{S}^k} I_{L_i^k}(L_j^{k-1}) > \gamma \right\} \quad (5)$$

Using γ this way means that the expansion of different sets can produce identical or overlapping results. For example, expanding either of the two sets $\{L_1^1\}$ or $\{L_1^1, L_2^1\}$ in Figure 6 with the default $\gamma = 0.5$ results in the identical set $\{L_1^0, L_2^0, L_3^0\}$. Accordingly, when traversing the hierarchy upwards, we need to identify and select one of the given sets. We contribute a solution for computing such a set, presented in Section 5.2.2.

Landmark Similarity. Besides using the AoI for selecting the landmarks used for expansion, the pairwise degree of overlap of the respective AoIs of two landmarks in \mathcal{L}^i with $i > 0$ defines the similarity between these two landmarks. By defining the similarity of the two landmarks in terms of the underlying neighborhood graph on the previous level the underlying manifold of the data is preserved even in the most abstract levels of the hierarchy. This notion of similarity is defined per level and thereby defines the mapping for the embedding per level. Therefore, the similarity cannot be directly computed when combining landmarks from different levels, as could be done for example by using Euclidean distances. We discuss ways to combine similarity sub-matrices from different levels in Section 5.2.3, fulfilling requirements V1–V3.

5.2. HSNE Extensions

To accommodate the integration of multiple HSNE levels into a single embedding and to allow a more fine-grained exploration we propose the following extensions to HSNE.

5.2.1. Landmark Selection

Here, instead of using a threshold on the number of terminated random walks, the user can directly specify the fraction of the landmarks on each level to proceed to the next level. In other words, based on a user specified threshold p the top p -th percentile of landmarks, according to the terminated random walks is chosen, resulting in a fixed reduction of $1 - p/100$ between two adjacent levels. Specifying the percentile is a more intuitive way of defining the granularity of the hierarchy and since the reduction is known at the time of computation the number of levels for the hierarchy can be computed automatically. In practice we typically observed reduction by approximately an order of magnitude in the original implementation, with the default hard threshold. Consequentially, setting $p = 90$ yields similar results. To allow a more fine grained exploration of the hierarchy, we set the default value to $p = 75$, meaning the number of landmarks is reduced to 25% between two adjacent levels. Even lower reduction rates are possible, however, they pose the risk of including uninformative landmarks.

5.2.2. Hierarchy Traversal

The proposed exploration of the HSNE hierarchy is much more fluent than the rather rigid original approach. Originally, every zoom operation results in an additional view and hierarchy traversal is strictly top-down. Here, a complete analysis session is carried out in a single embedding view. Typically, such a session will combine multiple instances of any of the workflows introduced in Section 2. As such, it will consist of subsequently setting the focus multiple times, adding and resolving a secondary focus, increasing and decreasing the LoD in different regions. Such a fluid interaction requires a more flexible handling of the traversal of the hierarchy.

In particular, HSNE does not provide means to zoom out. If less detail is required, one would need to find the corresponding previous view and continue exploration from there. As described in

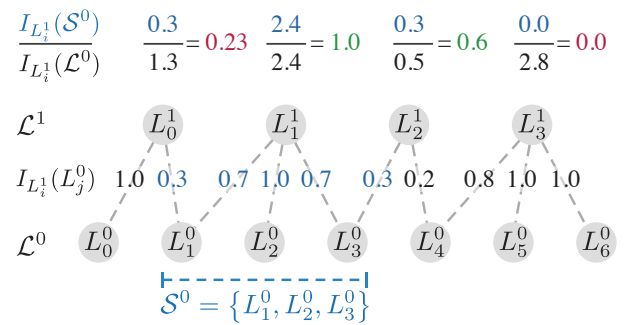


Figure 6: Example for Traversing the HSNE Hierarchy Upwards. To find the landmarks best representing the selection $\mathcal{S}^0 = \{L_1^0, L_2^0, L_3^0\}$ in \mathcal{L}^1 we compute the fractional influence $I_{L_i^1}(\mathcal{S}^0)$ for all landmarks and select those above a user-defined threshold. For example using 0.5 would yield $\mathcal{S}^1 = \{L_1^1, L_2^1\}$. Note that this is not the only possible set \mathcal{S}^1 as expanding L_1^1 alone would yield the same \mathcal{S}^0 .

Section 4.1.1 we implemented a tree structure, tracking the complete exploration. In most cases decreasing the LoD corresponds to reverting a previous increase of the LoD and therefore we can retrieve the less detailed representation directly by moving up in the existing tree structure. However, in rare cases it can be necessary to create a new group on a lower LoD. For example, when differentiating a focus that is already at the highest LoD, all contexts should be moved to a lower LoD that might not be in the tree.

As described in Section 5.1 there is not necessarily a unique solution to find the less detailed set \mathcal{S}^{k+1} corresponding to \mathcal{S}^k . In principal a minimal set can be found by testing out permutations of all involved landmarks. Such an approach could become very costly. Instead, we propose to approximate \mathcal{S}^{k+1} by computing the fraction of the influence of every landmark $L_i^{k+1} \in \mathcal{L}^{k+1}$ on the selected landmarks \mathcal{S}^k compared to its total influence.

$$I_{L_i^{k+1}}^{\text{norm}}(\mathcal{S}^k) = \frac{I_{L_i^{k+1}}(\mathcal{S}^k)}{I_{L_i^{k+1}}(\mathcal{L}^k)} \quad (6)$$

Here, $I_{L_i^{k+1}}(\mathcal{S}^k)$ is the total influence of the landmark L_i^{k+1} on the selection \mathcal{S}^k and $I_{L_i^{k+1}}(\mathcal{L}^k)$ the total influence of the same landmark on the complete level \mathcal{L}^k . We can then select the landmarks with a high relative influence on the selection, by thresholding on $I_{L_i^{k+1}}^{\text{norm}}$. We found experimentally that a threshold of 0.5, meaning more than half of the representation of a landmark corresponds to the current selection, creates small sets representing all of the input.

While the resulting set can be one of multiple possible solutions, in general it consists of the most important landmarks for the given input. We illustrate the example introduced in Section 5.1 in Figure 6. With $I_{L_i^{\text{norm}}} = 0.5$, decreasing the LoD of $\mathcal{S}^0 = \{L_1^0, L_2^0, L_3^0\}$ results in the corresponding set $\mathcal{S}^1 = \{L_1^1, L_2^1\}$. L_2^1 is not strictly necessary in \mathcal{S}^1 , as expanding only L_1^1 would produce the same \mathcal{S}^0 . However, in such cases the additional landmarks are of low impact (here $I_{L_2^1}(\mathcal{L}^0) = 0.5$) and in practice would rarely be selected as landmarks during the construction of the hierarchy. Furthermore, in an explorative setting the user would be able to probe the resulting embedding and inspect the similarity of the landmarks allowing them to identify such outliers.

5.2.3. Landmark Similarity

To compute the similarity embedding of the data points, combined from different levels of detail (LoDs), we first need to define the similarities between these points. While this could be done by directly computing the distances in the high-dimensional space, the resulting similarities would not reflect the non-linear distances preserved in the HSNE hierarchy. HSNE does provide a similarity matrix $\overline{\mathcal{L}^k \mathcal{L}^k}$ at each level of the hierarchy. However, it does not directly provide similarities for combinations of multiple LoDs. Here, we discuss ways to create a similarity matrix for combining multiple LoDs, underlying the similarity embedding.

One of the goals for the similarity embedding is that *the focus must use more space in the visualization* (requirement V1). As discussed in Section 5.1, HSNE defines the similarity of two points by the relative degree of overlap in their respective AoI. As the levels become smaller and the neighborhoods less detailed towards the higher levels of the hierarchy, the relative degree of overlap and

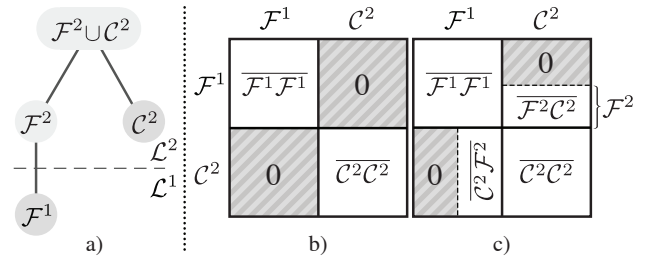


Figure 7: Distance Matrix Combination Modes for a basic Focus+Context graph shown in a). **Simple Combination**, b). Connections between focus and context are set to 0. **Pull-Up**, c). The focus is pulled up to the context level to extract the partial matrix between focus and context.

consequently the values for the similarity become larger. We can use this property to fulfill requirement V1, by creating the similarity matrix as a combination of partial similarity matrices from different levels. For points that shall occupy more space in the embedding (the focus), we take the partial similarity matrix from a more detailed level, while for points that shall occupy less space (the context) we take the partial similarity matrix from a less detailed level. In principal the result is a mixed matrix consisting of four partitions, the matrices for the focus, $\overline{\mathcal{F}^k \mathcal{F}^k}$, and context, $\overline{\mathcal{C}^l \mathcal{C}^l}$, as well as two blocks describing the similarities between focus and context $\overline{\mathcal{F}^k \mathcal{C}^l}$ and between context and focus $\overline{\mathcal{C}^l \mathcal{F}^k}$. Since the distances in HSNE are symmetric, $\overline{\mathcal{F}^k \mathcal{C}^l}$ is a rotated version of $\overline{\mathcal{C}^l \mathcal{F}^k}$. In case $l = k$ the matrix is identical to the similarity matrix of the union $\mathcal{F}^k \cup \mathcal{C}^l$. Using $\overline{\mathcal{F}^k \mathcal{F}^k}$ and $\overline{\mathcal{C}^l \mathcal{C}^l}$ from their respective levels guarantees that their structure in the combined embedding is as close as possible to the structure of the groups embedded separately.

Based on creating the similarity matrix through combination of partial matrices from different hierarchy levels, we propose two different modes, *Simple Matrix Combination* and *Pull-Up* to fulfill the competing requirements V2: *the focus must be separated from the context* and V3: *connections between focus and context should be maintained*.

Simple Matrix Combination. To achieve maximum separation between focus and context (requirement V2) we can simply set submatrices $\overline{\mathcal{F}^k \mathcal{C}^l}$ and $\overline{\mathcal{C}^l \mathcal{F}^k}$ to zero. This effectively cuts all inter-group connections and the embedding will separate the groups.

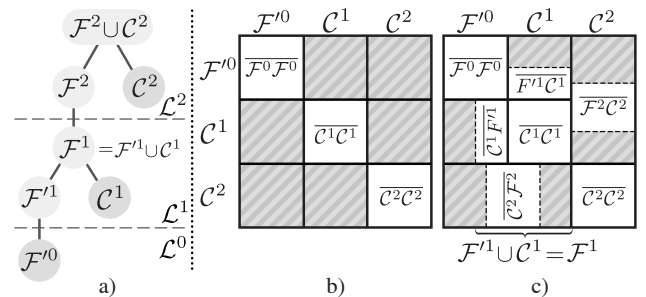


Figure 8: Distance Matrix Combination Modes with 3 levels of detail. A new focus was defined on \mathcal{F}^1 from Figure 7, a), resulting in the respective nested distance matrices in b) and c).

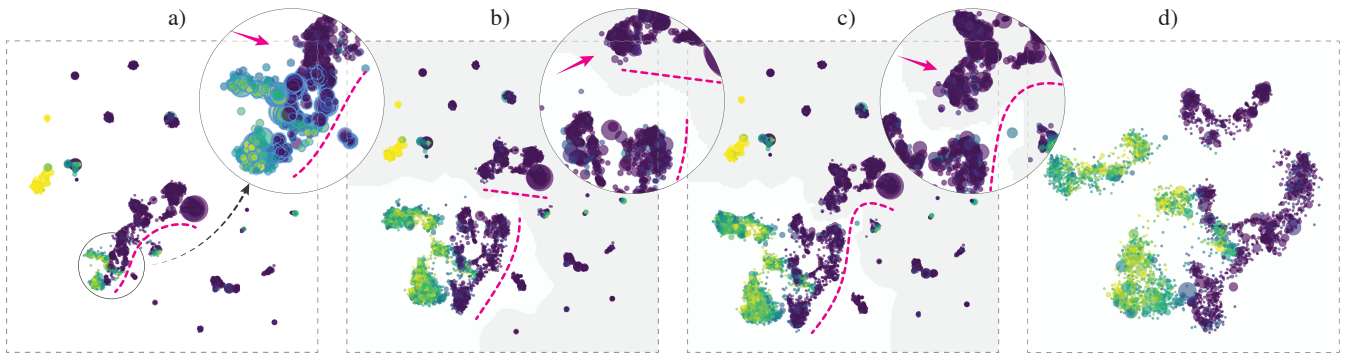


Figure 9: Comparison of Embeddings resulting from different matrix combination modes. A high-level embedding of a single-cell dataset [vULM*16] consisting of one million data points is shown in a). Computing the hierarchy took 4:20 minutes, but only needs to be done once. We focus on and differentiate the highlighted points (blue halos) in the inset of a) which are part of the larger structure indicated by the magenta line. The connection between focus and context is lost in the simple matrix combination mode in b) (the line illustrating the global structure breaks), in the pull up approach, c), the structure bends the context towards the focus, indicating the connection. Still, a clear separation between focus and context is preserved. Finally, d) shows only the focus landmarks embedded with standard HSNE. The structure is highly similar to the structure of the foci in b) and c). Starting from the embedding in a), computing b) and c) took 1:10 minutes. Computing the embedding in d) took slightly longer with 1:25 minutes, despite showing fewer data points. This is mostly caused by the fact that we initialized b) and c) with the previous embedding, while d) was computed from scratch, requiring more iterations until convergence.

Considering that we already have the similarity matrices per group, the most straight forward approach to do this simply concatenate these matrices. Figure 7a shows the basic Focus+Context tree with a single focus and context group, respectively. For this example the context \mathcal{C}^2 is taken from hierarchy level 2, while the focus \mathcal{F}^1 is one level more detailed. Figure 7b illustrates the combined similarity matrix for this approach.

Pull-Up Approach. To balance requirements V2 and V3, we need to sensibly fill $\overline{\mathcal{F}^k \mathcal{C}^l}$ and $\overline{\mathcal{C}^l \mathcal{F}^k}$. As described in Section 5.1 each less detailed level \mathcal{L}^k is a subset of the previous level \mathcal{L}^{k-1} . This means, we can find all points contained in \mathcal{L}^k in \mathcal{L}^{k-1} and, vice versa, some points contained in \mathcal{L}^{k-1} in \mathcal{L}^k . There are several ways to exploit this fact to construct a similarity matrix that considers interaction between focus and context.

Here, we propose to *pull-up* the focus to the context level and partially fill the empty part of the similarity matrix with those connections available in the context level. We start with the sub-matrices from the simple approach for the intra-group connections. Since we track the exploration in the Focus+Context tree, we can directly look-up \mathcal{F}^2 . With \mathcal{F}^2 , we can now extract the parts $\overline{\mathcal{F}^2 \mathcal{C}^2}$ and $\overline{\mathcal{C}^2 \mathcal{F}^2}$ of the similarity matrix from level 2 of the HSNE hierarchy. However, the landmarks that were added when zooming into \mathcal{L}^1 are not available in level 2 and therefore do not have connections to \mathcal{C}^2 . Figure 7c shows the resulting matrix.

For the examples in Figure 7 we used a simple graph with only one level difference between the focus and context. In practice the distance can vary, for example after applying multiple $d_+(\mathcal{F}^k)$ operations. Independent of the number of levels between the two groups, the matrix is constructed in the same way. For explorations with multiple context sets (Figure 8) the process of combining the similarity matrices is repeated iteratively. Independent of the mode we can simply replace the similarity matrix for the previ-

ous focus (here, $\overline{\mathcal{F}^1 \mathcal{F}^1}$) with a new sub-matrix that is constructed in the same way as described above.

Discussion. We found that the simple matrix combination method is very effective when the main goal is a strong separation between the focus and context groups while pull-up approach effectively balances requirements V2 and V3 while adhering to V1. For cases where we separated a cluster in focus and context groups, the groups stay close together at their separation points, but separate enough to not disturb the intrinsic focus partition (Figure 9c). The generally stronger connections from the less detailed hierarchy level effectively balance the connections missed for points that exist in \mathcal{F}^2 but not in \mathcal{F}^1 . For the pull-up approach we add some links between the focus and context groups by pulling the focus to the more abstract level of the context. In principal we can also push the context landmarks to the focus level without adding additional detail. This would allow us to fill the complete intra-group sub-matrices. We expected that adding such a large amount of connections weakens the separation between the groups too much. We implemented two methods based on pulling down the context and could indeed observe undesired mixing in experiments. All methods introduce some distortion, as compared to embedding data from a single LoD, only. For the simple matrix combination this distortion is between groups and easy to identify. The introduction of links between groups in the pull-up approach can additionally lead to distortions within a group, as only some landmarks within a group will be connected to another group. If such landmarks are weakly connected within their specific groups, they could be pulled out of their respective group. In practice, however, we noticed that this rarely happens as the landmarks that are connected to other groups are also strongly connected within their respective groups, as this was a criteria to select them as landmarks initially. This can also be seen in the examples in Figure 9 where the structure of the foci in Figure 9b and Figure 9c is very similar to the original HSNE embedding of the focus only in Figure 9d.

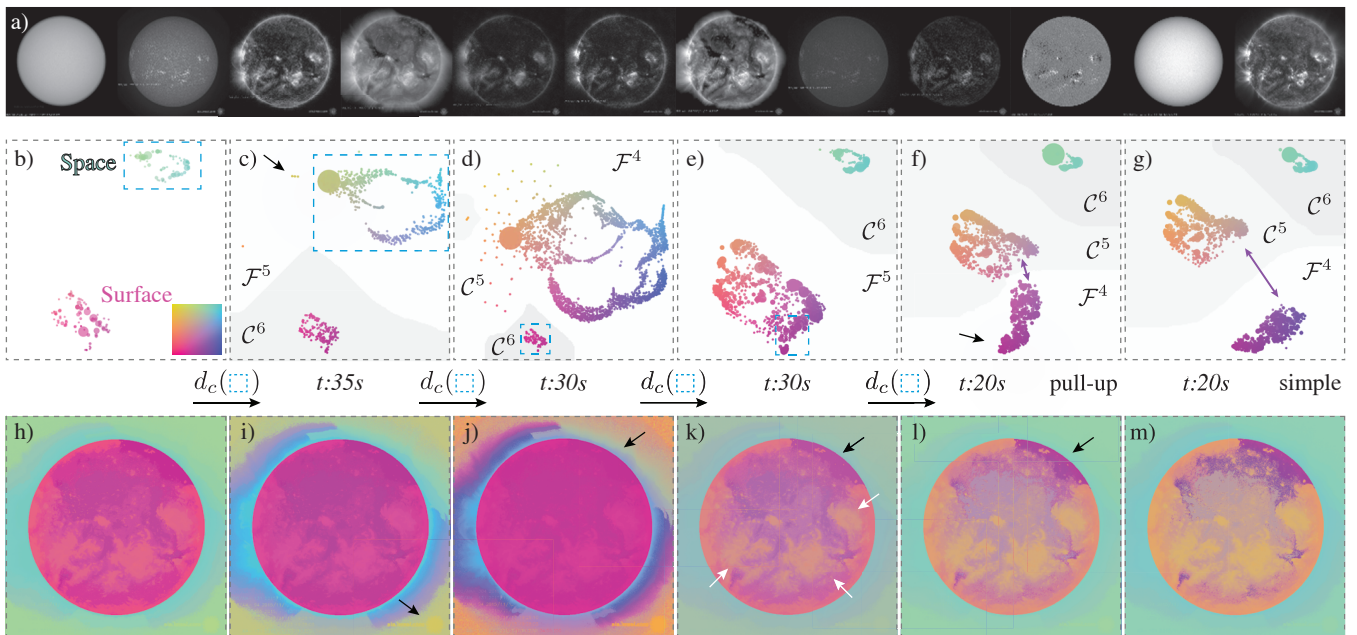


Figure 10: Example of a Focus+Context Exploration with HSNE. The input data are shown in a). Each of the images corresponds to one dimension. Focus+Context HSNE embeddings shown in b) to g). Landmarks are colored according to their (x,y)-coordinates in the embedding using the 2D colormap shown in b). Required computation time to achieve the presented results shown below the embeddings. Images with pixels colored according to their corresponding landmarks shown in h) to m).

5.3. Implementation

We extended the open source [High Dimensional Inspector](#) library to allow the described seamless traversal of the hierarchy in both directions. The prototype for illustrating the interaction design is implemented in Cytosplore [HPvU*16, vUHP*17]. The library and application are implemented in C++. Computation of the hierarchy and embeddings are performed with the original HSNE library. For a detailed analysis of the computational performance we refer to our previous work on the HSNE algorithm itself [PHL*16]. Typically a Focus+Context embedding will converge slightly faster since we initialize it with the previous positions, whereas the original HSNE creates a new embedding that is initialized randomly. On the other hand, some of this gain will be offset by the fact that the context adds additional landmarks to the embedding compared to the standard HSNE of only the focus selection. For an intuition, we provide computation times for the examples in [Figure 9](#) and [Figure 10](#). All measurements were taken using a quad core intel core i7 6820HQ at 2.7Ghz with all data in working memory. We use OpenGL for fast rendering of the embeddings and to derive the topographical maps for visualizing the level of detail on-the-fly, directly during the optimization.

6. Use Case

To illustrate the effectiveness of Focus+Context HSNE, we follow a use case of the original work by Pezzotti et al. [PHL*16] on the exploration of hyperspectral images of the sun. We use the same data-set as presented in the original work, downloaded from the [Solar Dynamics Observatory](#). The dataset consists of twelve dimensions, represented each by a gray-scale image, corresponding to different spectral regions ([Figure 10a](#)). The image resolution is $1,024 \times 1,024$. We consider every pixel a twelve-dimensional

data point, resulting in roughly one million data points as input to HSNE. An illustration of the original exploration is shown in the original publication [PHL*16, Figure 6]. As indicated in [Section 2](#), originally, the low-detail overview embedding is explored first, by probing different regions of the embedding. Selecting a region in the embedding highlights the corresponding pixels in an image view. After identifying and zooming into two regions of interest, the more detailed plots are displayed separately in new views and further exploration and probing is limited to these sub-regions.

Here, in addition to using the presented Focus+Context approach for the exploration, we augment the visualization in image space by recoloring. Cheng et al. [CXM18] present recoloring of multi-dimensional images, based on an optimized 2D projection, here we follow a similar approach, but use the (x,y) coordinates in the embedding, as shown by Abdelmoula et al. [APH*18]. When inspecting the embedding and image views, the user needs to be able to identify the origin of pixels in the HSNE map and compare different pixels according to their origin. Furthermore, we do not want to steer attention with the colormap. Therefore, we picked several colormaps that provide a reasonable compromise between tasks ER2, ER3, SR2 presented by Bernard et al. [BSM*15, Table 3]. For the example in [Figure 10](#), we chose the Mittelstädt et al. colormap [SBM*14]. In the implemented prototype we allow the user to choose between the Bremm et al. regular and stretched [BLBS11], TeulingFig3NoWhitening [TSS11], and the presented Mittelstädt et al. colormaps. We extracted the colormaps from ColorMap-Explorer [SBT*15].

The exploration starts with a single-level-of-detail embedding shown in [Figure 10b](#). Landmarks are drawn as semi-transparent circles, the size corresponding to their influence on the lower level and

the color corresponding to their location in the plot. We can immediately identify two main groups in this plot. Comparing the spatial representation in Figure 10h we can see that the two groups correspond to the surface of the sun (pink) and the space (green). While some more fine-grained structure can already be identified at this LoD the main focus here is on the separation of the two groups.

Following the example of Pezzotti et al. [PHL*16], we first want to inspect the space cluster in the embedding. Therefore, we select this cluster and create and differentiate the focus, $d_c(\odot)$. The resulting embedding is shown in Figure 10c and the corresponding image in Figure 10i. We can see that the embedding behaves as desired, leading to a more compact representation of the context, \mathcal{C} , while the focus, \mathcal{F} , becomes larger and more detailed. A curious detail shown in the original work becomes visible here. A small group of points (arrow in Figure 10c) separates from the main group. Comparing the image view, we see that this cluster corresponds to the overlaid AIA-logo. We create a new focus, excluding this group, and differentiate, $d_c(\odot)$, resulting in the embedding in Figure 10d. Now the focus strongly dominates the plot, while the context groups are again more compact. As a result the surface now hardly shows any structure in the image view Figure 10j, leading the attention to the increased structure in the focus. Here, we can now clearly see the layered structure of the corona by its color from deep purple to light blue. Two strong sunflares can be identified on the left side of the image in blue, while areas with reduced activity show up on the top right (arrow) and bottom.

In the next step we want to investigate the surface in more detail. Thanks to the proposed Focus+Context interaction model we can simply select the corresponding landmarks in Figure 10d and call set focus & differentiate, $d_c(\odot)$. As described in Section 4 the selection now becomes the new focus, one level more detailed than its initial level, while the remaining data becomes the context and is moved back up to the initial LoD. The resulting embedding (Figure 10e) now assigns much more space to the surface group, while the space group collapses to a much smaller region. We can already see more detail on the sun surface (Figure 10k). Hotter regions are on the lower-right part in the embedding, resulting in a purple color in the image view, while orange parts correspond to lower temperature regions. In particular, three active regions on the surface start to appear (Figure 10k, white arrows). The same differentiation had been observed by Pezzotti et al. [PHL*16]. Finally, we select a small region on the bottom part as the new focus and differentiate, $d_c(\odot)$. We can now clearly see that the purple area corresponds in large part to a large low-temperature area on the top right of the surface, corresponding to an area that also showed clear differentiation in the corona (black arrows in Figure 10j–10l). For computing the combined similarity matrix, we used the pull-up approach as described in Section 5.2.3. As indicated by the purple arrow in Figure 10f the points in the focus area are still in close proximity to the points they were separated from during selection. For comparison we show the same focus and context groups with the similarity matrix combined with the simple approach in Figure 10g. Here, the new focus is completely separated from its origin. While the recolored images (Figure 10l and 10m) show very similar structure, the connection between the surface context and focus groups is lost in the embedding with the simple approach. In most cases the pull-up approach, preserving this information, should be preferred.

7. Conclusion

We have presented a framework, including an interaction model and visual design for Focus+Context exploration of hierarchical embeddings. We extended the hierarchical dimensionality reduction technique HSNE to support the proposed model. We have demonstrated its effectiveness in an exemplary use case on hyperspectral images. In particular, incorporating the Focus+Context concept directly into the mapping of the dimensionality reduction by combining similarity matrices from different levels of detail, is a natural fit for non-linear embeddings. This approach can be tuned by selecting the type of similarity matrix combination.

While our extensions to the HSNE hierarchy allow for a much more fine-grained exploration compared to the original implementation, the depth of a zoom operation is left to be specified by the user. A future research direction could be to optimize the levels according to the available space. For example, skipping several levels during the differentiate operation while reducing detail of the context at the same time. We illustrate a brief case study for the exploration of multi-dimensional images in Section 6. The application of the presented techniques to real-world data exploration tasks alongside a structured evaluation for these tasks provide open questions for future work.

Acknowledgements. This work was partially funded through NWO projects 12720, *VAnPIRe*, and 12721, *Genes in Space*, and the VIDI project (#813558) on *Visual Data Science for Imaging Biomarker Discovery*, supported by the Trond Mohn Foundation in Bergen.

References

- [AEGEALM07] AGARWAL A., EL-GHAZAWI T., EL-ASKARY H., LEMOIGNE J.: Efficient hierarchical-pca dimension reduction for hyperspectral imagery. In *2007 IEEE International Symposium on Signal Processing and Information Technology* (2007), pp. 353–356. doi: 10.1109/ISSPIT.2007.4458191. 3
- [APH*18] ABDELMOULA W. M., PEZZOTTI N., HÖLLT T., DIJKSTRA J., VILANOVA A., McDONNELL L. A., LELIEVELDT B.: Interactive visual exploration of 3d mass spectrometry imaging data using hierarchical stochastic neighbor embedding reveals spatiomolecular structures at full data resolution. *Journal of Proteome Research* 17, 3 (2018), 1054–1064. doi:10.1021/acs.jproteome.7b00725. 9
- [BG06] BORG I., GROENEN P.: Modern multidimensional scaling: Theory and applications. *Journal of Educational Measurement* 40, 3 (2006), 277–280. doi:10.1111/j.1745-3984.2003.tb01108.x. 1
- [BLBS11] BREMM S., LANDEBERGER T. V., BERNARD J., SCHRECK T.: Assisted descriptor selection based on visual comparative data analysis. *Computer Graphics Forum* 30, 3 (2011), 891–900. doi: 10.1111/j.1467-8659.2011.01938.x. 9
- [BSIM14] BREHMER M., SEDLMAIR M., INGRAM S., MUNZNER T.: Visualizing dimensionally-reduced data: Interviews with analysts and a characterization of task sequences. In *Proceedings of ACM BELIV Workshop* (2014), pp. 1–8. doi:10.1145/2669557.2669559. 3
- [BSM*15] BERNARD J., STEIGER M., MITTELSTÄDT S., THUM S., KEIM D., KOHLHAMMER J.: A survey and task-based quality assessment of static 2d colormaps. In *SPIE Proceedings on Visualization and Data Analysis* (2015), vol. 9397. doi:10.1117/12.2079841. 9
- [CKB09] COCKBURN A., KARLSON A., BEDERSON B. B.: A review of overview+detail, zooming, and focus+context interfaces. *ACM Computing Surveys* 41, 1 (2009), 2:1–2:31. doi:10.1145/1456650.1456652. 1, 3
- [CXM18] CHENG S., XU W., MUELLER K.: Colormapnd: A data-driven

- approach and tool for mapping multivariate data to color. *IEEE Transactions on Visualization and Computer Graphics* (2018), 1–1. doi:10.1109/TVCG.2018.2808489. 9
- [EHH12] ENGEL D., HÜTTENBERGER L., HAMANN B.: A survey of dimension reduction methods for high-dimensional data analysis and visualization. In *Visualization of Large and Unstructured Data Sets: Applications in Geospatial Planning, Modeling and Engineering - Proceedings of IRTG 1131 Workshop 2011* (2012), vol. 27, pp. 135–149. doi:10.4230/OASIScs.VLUDS.2011.135. 1
- [Fur99] FURNAS G. W.: The fisheye view: A new look at structured files. In *Readings in Information Visualization*, Card S. K., Mackinlay J. D., Shneiderman B., (Eds.). Morgan Kaufmann Publishers Inc., 1999, pp. 312–330. 1
- [Hau06] HAUSER H.: Generalizing focus+context visualization. In *Scientific Visualization: The Visual Extraction of Knowledge from Data*, Bonneau G.-P., Ertl T., Nielson G. M., (Eds.). Springer Berlin Heidelberg, 2006, pp. 305–327. 1
- [HPvU*16] HÖLLT T., PEZZOTTI N., VAN UNEN V., KONING F., EISEMANN E., LELIEVELDT B. P. F., VILANOVA A.: Cytosplore: Interactive immune cell phenotyping for large single-cell datasets. *Computer Graphics Forum (Proceedings of EuroVis)* 35, 3 (2016), 171–180. doi:10.1111/cgf.12893. 9
- [HPvU*18] HÖLLT T., PEZZOTTI N., VAN UNEN V., KONING F., LELIEVELDT B., VILANOVA A.: Cyteguide: Visual guidance for hierarchical single-cell analysis. *IEEE Transactions on Visualization and Computer Graphics* 24, 1 (2018), 739 – 748. doi:10.1109/TVCG.2017.2744318. 2, 3
- [JPLL01] JANNÉ K., PETTERSEN J., LINDBERG N.-O., LUNDSTEDT T.: Hierarchical principal component analysis (pca) and projection to latent structure (pls) technique on spectroscopic data as a data pretreatment for calibration. *Journal of Chemometrics* 15, 4 (2001), 203–213. doi:10.1002/cem.677. 3
- [LGM*18] LEITE R. A., GSCHWANDTNER T., MIKSCH S., KRIGLSTEIN S., POHL M., GSTREIN E., KUNTNER J.: EVA: Visual analytics to identify fraudulent events. *IEEE Transactions on Visualization and Computer Graphics* 24, 1 (2018), 330–339. doi:10.1109/TVCG.2017.2744758. 1
- [LvUH*18] LI N., VAN UNEN V., HÖLLT T., THOMPSON A., VAN BERGEN J., PEZZOTTI N., EISEMANN E., VILANOVA A., CHUVA DE SOUSA LOPES S. M., LELIEVELDT B. P., KONING F.: Mass cytometry reveals innate lymphoid cell differentiation pathways in the human fetal intestine. *Journal of Experimental Medicine* 215, 5 (2018), 1383–1396. doi:10.1084/jem.20171934. 1
- [MCCD13] MIKOLOV T., CHEN K., CORRADO G., DEAN J.: Efficient estimation of word representations in vector space. In *Proceedings of Workshop at International Conference on Learning Representations (ICLR)* (2013), pp. 1310–1318. 1
- [Mun14] MUNZNER T.: *Visualization Analysis and Design: Principles, Techniques, and Practice*, 1 ed. Taylor & Francis Inc., 2014. 1, 2, 3
- [OKB*08] ORNATSKY O. I., KINACH R., BANDURA D. R., LOU X., TANNER S. D., BARANOV V. I., NITZ M., WINNIK M. A.: Development of analytical methods for multiplex bio-assay with inductively coupled plasma mass spectrometry. *Journal of Analytical Atomic Spectrometry* 23 (2008), 463–469. doi:10.1039/B710510J. 1
- [PHL*16] PEZZOTTI N., HÖLLT T., LELIEVELDT B. P. F., EISEMANN E., VILANOVA A.: Hierarchical stochastic neighbor embedding. *Computer Graphics Forum (Proceedings of EuroVis)* 35, 3 (2016), 21–30. doi:10.1111/cgf.12878. 1, 2, 3, 5, 9, 10
- [PHvG*18] PEZZOTTI N., HÖLLT T., VAN GEMERT J., LELIEVELDT B., EISEMANN E., VILANOVA A.: Deepeyes: Progressive visual analytics for designing deep neural networks. *IEEE Transactions on Visualization and Computer Graphics* 24, 1 (2018), 98 – 108. doi:10.1109/TVCG.2017.2744358. 1
- [PM08] PAULOVICH F. V., MINGHIM R.: HiPP: A novel hierarchical point placement strategy and its application to the exploration of document collections. *IEEE Transactions on Visualization and Computer Graphics* 14, 6 (2008), 1229–1236. doi:10.1109/TVCG.2008.138. 1, 3
- [PNML08] PAULOVICH F. V., NONATO L. G., MINGHIM R., LEVKOWITZ H.: Least square projection: A fast high-precision multidimensional projection technique and its application to document mapping. *IEEE Transactions on Visualization and Computer Graphics* 14, 3 (2008), 564–575. doi:10.1109/TVCG.2007.704443. 2, 3
- [SBM*14] STEIGER M., BERNARD J., MITTELSTÄDT S., LÜCKE-TIEKE H., KEIM D., MAY T., KOHLHAMMER J.: Visual analysis of time-series similarities for anomaly detection in sensor networks. *Computer Graphics Forum* 33, 3 (2014), 401–410. doi:10.1111/cgf.12396. 9
- [SBT04] SILVA V., B. TENENBAUM J.: *Sparse Multidimensional Scaling using Landmark Points*. Tech. rep., Stanford University, 2004. 3
- [SBT*15] STEIGER M., BERNARD J., THUM S., MITTELSTÄDT S., HUTTER M., KEIM D. A., KOHLHAMMER J.: Explorative analysis of 2d color maps. In *23rd International Conference in Central Europe on Computer Graphics, Visualization and Computer Vision* (2015), pp. 151–160. 9
- [SMT13] SEDLMAIR M., MUNZNER T., TORY M.: Empirical guidance on scatterplot and dimension reduction technique choices. *IEEE Transactions on Visualization and Computer Graphics* 19, 12 (2013), 2634–2643. doi:10.1109/TVCG.2013.153. 3
- [SSTR93] SARKAR M., SNIBBE S. S., TVERSKY O. J., REISS S. P.: Stretching the rubber sheet: A metaphor for viewing large layouts on small screens. In *Proceedings of the 6th Annual ACM Symposium on User Interface Software and Technology* (1993), pp. 81–91. doi:10.1145/168642.168650. 1
- [SZS*17] SACHA D., ZHANG L., SEDLMAIR M., LEE J. A., PELTONEN J., WEISKOPF D., NORTH S. C., KEIM D. A.: Visual interaction with dimensionality reduction: A structured literature analysis. *IEEE Transactions on Visualization and Computer Graphics* 23, 1 (2017), 241–250. doi:10.1109/TVCG.2016.2598495. 3
- [TSS11] TEULING A. J., STÖCKLI R., SENEVIRATNE S. I.: Bivariate colour maps for visualizing climate data. *International Journal of Climatology* 31, 9 (2011), 1408–1412. doi:10.1002/joc.2153. 9
- [vdMH08] VAN DER MAATEN L., HINTON G.: Visualizing data using t-SNE. *Journal of Machine Learning Research* 9 (2008), 2579–2605. 1, 3, 5
- [vUHP*17] VAN UNEN V., HÖLLT T., PEZZOTTI N., LI N., REINDERS M. J. T., EISEMANN E., KONING F., VILANOVA A., LELIEVELDT B. P. F.: Visual analysis of mass cytometry data by hierarchical stochastic neighbor embedding reveals rare cell types. *Nature Communications* 8, 1740 (2017), 1–10. doi:10.1038/s41467-017-01689-9. 5, 9
- [vULM*16] VAN UNEN V., LI N., MOLENDIJK I., TEMURHAN M., HÖLLT T., VAN DER MEULEN-DE JONG A. E., VERSAPAGET H. W., MEARIN M. L., MULDER C. J., VAN BERGEN J., LELIEVELDT B. P. F., KONING F.: Mass cytometry of the human mucosal immune system identifies tissue- and disease-associated immune subsets. *Immunity* 44, 5 (2016), 1227–1239. doi:10.1016/j.immuni.2016.04.014. 8
- [WKM98] WESTERHUIS J. A., KOURTI T., MACGREGOR J. F.: Analysis of multiblock and hierarchical pca and pls models. *Journal of Chemometrics* 12, 5 (1998), 301–321. doi:10.1002/(SICI)1099-128X(199809/10)12:5<301::AID-CEM515>3.0.CO;2-S. 3
- [WM04] WILLIAMS M., MUNZNER T.: Steerable, progressive multidimensional scaling. In *IEEE Symposium on Information Visualization* (2004), pp. 57–64. 3
- [WWZ*19] WANG Y., WANG Y., ZHANG H., SUN Y., FU C.-W., SEDLMAIR M., CHEN B., DEUSSEN O.: Structure-aware fisheye views for efficient large graph exploration. *IEEE Transactions on Visualization and Computer Graphics* 25, 1 (2019), 566–575. doi:10.1109/TVCG.2018.2864911. 2